Age-Severity Relationships in Families Linked to *FCD2* with Retroillumination Photography

Elyse J. McGlumphy,[1] *William S. Yeo,*[1] *S. Amer Riazuddin,*[2] *Amr Al-Saif,*[2] *Jiangxia Wang,*[3] *Allen O. Eghrari,*[1] *Danielle N. Meadows,*[1] *David G. Emmert,*[1] *Nicholas Katsanis,*[4] *and John D. Gottsch*[1]

Purpose. Fuchs corneal dystrophy (FCD) is a progressive disorder of the corneal endothelium and is pathologically defined by the presence of guttae, which are excrescences of the Descemet membrane. The present study was undertaken to investigate the age-severity relationship of the *FCD2*-linked disease phenotype using retroillumination photography and to compare it with the characteristics of *FCD1*.

Methods. Two large families with multiple affected members were recruited. Exclusion analyses of the known late-onset FCD loci were completed with closely spaced STR markers, whereas genes associated with early- and late-onset FCD were investigated by bidirectional sequencing. Haplotypes were constructed, and two-point LOD scores were calculated. To document age-severity relationships, retroillumination photographs were acquired from members of both families.

Results. Parametric linkage and haplotype analysis mapped both families to *FCD2* with significant two-point LOD scores. A total of 70,249 guttae were counted in 14 persons from both families. A significant increase in guttae density in the inferotemporal region ($P = 0.016$) was observed, a pattern similarly observed in a family linked to *FCD1*. Similarly, *FCD2*-linked families display an exponential trend in severity with age, as was observed in a family linked to *FCD1*. Finally, comparison of *FCD1* and *FCD2* exponential models suggested that the *FCD1* phenotype is significantly more severe ($P = 0.01$).

Conclusions. A combination of genetic mapping and retroillumination photography was used to quantify the severity of the disease phenotype associated with *FCD2* and to compare it to the disease characteristics of *FCD1*. These data suggest that this approach might have sufficient resolution to discriminate between discrete genetic FCD backgrounds, which will potentially aid in patient management. (*Invest Ophthalmol Vis Sci.* 2010;51:6298–6302) DOI:10.1167/iovs.10-5187

From the [1]Center for Corneal Genetics, Cornea and External Disease Service, The Wilmer Eye Institute, Johns Hopkins University School of Medicine, Baltimore, Maryland; [2]McKusick-Nathans Institute of Genetic Medicine, Johns Hopkins University School of Medicine, Baltimore, Maryland; [3]Department of Biostatistics, Johns Hopkins Bloomberg School of Public Health; and [4]Center for Human Disease Modeling, Department of Cell Biology, Duke University, Durham, North Carolina.

Supported by National Eye Institute Grant R01EY016835 (JDG). Data analysis was supported by Wilmer Biostatistics Core Grant R01EY01765. NK is Distinguished George W. Brumley Professor. JDG is the Margaret C. Mosher Professor of Ophthalmology.

Submitted for publication January 8, 2010; revised March 30 and May 24, 2010; accepted June 9, 2010.

Disclosure: **E.J. McGlumphy**, None; **W.S. Yeo**, None; **S.A. Riazuddin**, None; **A. Al-Saif**, None; **J. Wang**, None; **A.O. Eghrari**, None; **D.N. Meadows**, None; **D.G. Emmert**, None; **N. Katsanis**, None; **J.D. Gottsch**, None

Corresponding author: John D. Gottsch, Center for Corneal Genetics, Cornea and External Disease Service, The Wilmer Eye Institute, The Johns Hopkins Hospital, 600 N. Wolfe Street, Baltimore, MD 21287; jgottsch@jhmi.edu.

Fuchs corneal dystrophy (FCD) is an inheritable, progressive disorder of the corneal endothelium that affects approximately 4% of the population older than 40 years in the Western world.[1,2] Typified by stromal edema and decreasing visual integrity, FCD leads to the overall progressive loss of corneal endothelial function and contributes significantly to the total number of corneal transplantations in the United States.[3] Phenotypically, FCD is characterized by the presence of corneal guttae, histologically defined as drop-like excrescences of Descemet membrane, the collagen-rich basal lamina of the corneal endothelium.[4,5]

FCD is genetically heterogeneous, exhibiting an autosomal dominant mode of inheritance with variable penetrance and expressivity. The rare form of early-onset FCD is causally associated with mutations in *COL8A2*, whereas the more common late-onset FCD has been localized to four loci, *FCD1, FCD2, FCD3*, and *FCD4* on chromosomes 13, 18, 5, and 9, respectively.[6–11] In addition, recent data have indicated that late-onset FCD overlaps genetically with earlier forms of clinically distinct corneal dystrophies. Mutational analysis and subsequent functional evaluations showed that, in contrast to null alleles in the transcription factor *TCF8* that cause posterior polymorphous corneal dystrophy, missense changes can cause adult-onset FCD.[11,12] Similarly, heterozygous mutations in *SLC4A11*, a gene mutated in recessive congenital hereditary corneal dystrophy, have been found in patients with late-onset FCD.[13]

Aside from the clinical and morphologic differences noted in L450W *COL8A2* early-onset and late-onset FCD, there are no reports of differences in presentation among FCD contributing loci and genes using retroillumination photography. Retroillumination photography is an effective means to document and quantify corneal guttae, and using this technique we previously have shown an exponential age-severity relationship in a family linked to *FCD1*.[14,15] Here, we investigate the age-severity relationship in *FCD2*-linked families, document the distribution of corneal guttae with retroillumination photography, and compare the characteristics of the *FCD1* and *FCD2* disease phenotypes.

Methods

Recruitment

Two late-onset FCD families were recruited through the Cornea and External Disease Service at the Wilmer Eye Institute. All participating individuals were examined by means of slit-lamp biomicroscopy. Affectation status and severity of disease was determined using the scale proposed by Krachmer et al.[2] Positive disease status was indicated if the patient had a minimum grading score of 1, which represents 12 or more central nonconfluent guttae in at least one eye.

The study protocol was approved by the Joint Committee on Clinical Investigation at The Johns Hopkins University School of Medicine and was conducted in accordance with the tenets of the Declaration of Helsinki. Informed written consent was obtained from all participants after explanation of the nature and potential consequences of the study. Blood samples (10–15 mL each) were collected from both affected and unaffected members, and genomic DNA was extracted from white blood cells (Gentra Puregene Blood Kit; Qiagen Inc., Valencia, CA).

Exclusion Analyses of Late-Onset FCD Loci

Exclusion analyses were performed with fluorescence-labeled short tandem repeat (STR) markers spanning the critical intervals of *FCD1*, *FCD2, FCD3,* and *FCD4*. Primer sequences amplifying the short tandem repeats are as reported previously.[8–11] Multiplex polymerase chain reactions (PCRs) were carried out in a thermocycler (ABI 9700; Applied Biosystems, Foster City, CA). Briefly, each reaction was carried out in a 5-μL mixture containing 40 ng genomic DNA, various combinations of 10 μM-dye-labeled primer pairs, 0.5 μL 10× buffer (GeneAmp PCR Buffer II; Applied Biosystems), 0.5 μL 10 mM dNTP mix (GeneAmp PCR Buffer II; Applied Biosystems), 2.5 mM $MgCl_2$, and 0.2 U *Taq* DNA polymerase (AmpliTaq; Applied Biosystems). Amplification was performed in a PCR system (GeneAmp PCR System 9700; Applied Biosystems). Initial denaturation was carried out for 5 minutes at 95°C, followed by 10 cycles of 15 seconds at 94°C, 15 seconds at 55°C, and 30 seconds at 72°C, and then by 20 cycles of 15 seconds at 89°C, 15 seconds at 55°C, and 30 seconds at 72°C. The final extension was performed for 10 minutes at 72°C and was followed by a final hold at 4°C. PCR products from each DNA sample were pooled and mixed with a loading cocktail containing HD-400 size standards (Applied Biosystems). The resultant PCR products were separated in a DNA sequencer (ABI 3100; Applied Biosystems) and were analyzed with special software (GENESCAN 4.0 software; Applied Biosystems). These alleles were used to construct disease haplotypes for each family and were inspected visually. Results of haplotype analyses were further confirmed with two-point parametric LOD scores.

Linkage Analyses

Two-point linkage analyses were performed with the FASTLINK version of MLINK from the LINKAGE Program Package (provided in the public domain by the Human Genome Mapping Project Resources Centre, Cambridge, UK),[16,17] under an autosomal dominant model with a 0.02 disease allele frequency and 90% penetrance. The marker order and distances between the markers were obtained from the Marshfield database and the NCBI sequence maps. Allele frequencies were derived from 96 unrelated and unaffected persons.

Exclusion of *SLC4A11* and *TCF8*

SLC4A11 and *TCF8* were excluded through bidirectional sequencing of the coding exons and exon-intron boundaries of these genes. Primer pairs for *SLC4A11* and *TCF8* were designed using the primer3 program (http://fokker.wi.mit.edu/primer3/).[18] Sequences and annealing temperatures are available on request. Amplifications were performed in 25-μL reactions containing 50 ng genomic DNA, 400 nM each primer, 250 μM dNTPs, 2.5 mM $MgCl_2$, and 0.2 U *Taq* DNA polymerase in the standard PCR buffer provided by the manufacturer (Applied Biosystems). PCR amplification consisted of a denaturation step at 96°C for 5 minutes followed by 40 cycles, each consisting of 96°C for 30 seconds followed by 57°C (or primer set-specific annealing temperature) for 30 seconds and 72°C for 1 minute. PCR products were analyzed on a 2% agarose gel and purified by ethanol precipitation. PCR primers for each exon were used for bidirectional sequencing using reaction mix (BigDye Terminator Ready; Applied Biosystems) according to the manufacturer's instructions. Sequencing products were precipitated and resuspended in 10 μL formamide (Applied Biosystems) and denatured at 95°C for 5 minutes. Sequencing was performed on an automated sequencer (ABI Prism 3100; Applied Biosystems), and sequencing results were assembled with sequencing analysis software (ABI Prism version 3.7; Applied Biosystems) and analyzed with reference-based analysis software (SeqScape; Applied Biosystems).

Retroillumination Images

Retroillumination images were acquired from positive *FCD2*-linked persons. Each person underwent bilateral pupil dilation prior to retroillumination photography, and retroillumination images were obtained with a photo slit-lamp biomicroscope (Haag-Streit Model BQ900, Haag-Streit International, Koeniz, Switzerland) and were acquired with a camera (D2xs; Nikon Corporation, Tokyo, Japan) equipped with a magnification changer. The flash power averaged 460 W (range, 240–720 W), and camera aperture was set between f32 and f44. A minimum of four photos was obtained for each eye (two per opposite orientation of the retroillumination beam).

Statistical Analysis

Retroillumination images were processed (Photoshop CS4 Extended Package; Adobe Systems, Inc., San Jose, CA) as described.[15] In brief, a circular grid with 12 diagonal and eight concentric sections was superimposed on each image, dividing the cornea into a total of 96 sampled sectors. Individual guttae in each sector were identified and summated manually on a computer (Photoshop Count Analysis; Adobe Systems, Inc.), and the total counts were exported to a spreadsheet (Excel; Microsoft Corp., Redmond, WA) for data analysis. Differences in superior versus inferior or nasal versus temporal distribution of guttae were then assessed through statistical comparison of symmetrically opposing quadrants, as described previously.[15] A log-linear regression on the number of guttae was performed to regress the log of number of guttae and to examine the age-severity trend for families linked to *FCD1* and *FCD2*. Linear combinations of the regression estimates were performed to compare the age-severity relationships from the two groups (STATA version 11.0; StataCorp, College Station, TX).[19,20]

Results

We recruited two late-onset FCD families of northern European descent. All participants in both families were examined for corneal guttae with a slit lamp biomicroscope, and 23 persons in both families fulfilled the criterion for being designated as affected: FCD Krachmer grading of +1 or higher (Table 1). Family structure and segregation pattern of the disease phenotype in both families was consistent with an autosomal dominant mode of inheritance (Fig. 1). In family MO, nine affected members (7 females, 2 males) and 10 unaffected members

Table 1. Total Number of Guttae and Fuchs Krachmer Grading of *FCD2*-Linked Affected MO and PA Family Members

Family Member	Age (y)	Sex	Total No. of Guttae (both eyes)	Krachmer Grading (OD/OS)
PA-III:11	34	M	1707.5	2.5/2.5
MO-III:10	37	F	426	1.0/1.5
PA-III:7	38	F	2914.5	1.5/2.0
PA-III:18	44	F	3303.5	1.0/trace
PA-III:8	44	F	1727.5	2.5/2.75
PA-III:6	47	F	1628	2.0/2.5
PA-III:5	48	F	2162	2.5/2.0
MO-III:5	50	F	988	1.0/1.5
PA-III:10	52	M	19536.5	4.0/4.0
PA-III:9	53	M	3743.5	3.0/3.0
MO-III-4	56	F	3273	2.0/2.5
MO-II:15	65	M	18510	4.0/4.0
PA-II:9	66	F	4226	3.5/3.5
MO-II:3	83	M	6103	4.5/4.0

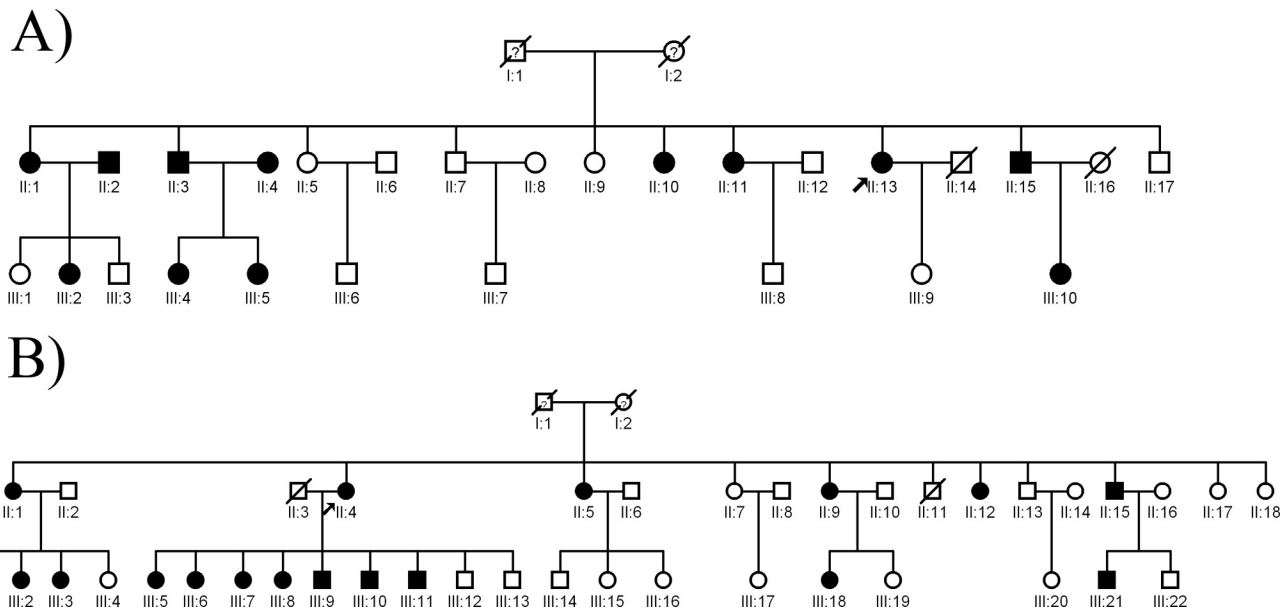

Figure 1. Pedigrees of the families linked to *FCD2*. (**A**) Family MO. (**B**) Family PA. *Squares*: male; *Circles*: female; *Filled symbols*: positive affectation status; *Empty symbols*: negative affectation status; *Diagonal line through a symbol*: deceased; *Arrow next to a symbol*: proband; *Question mark in a symbol*: disease status unknown.

agreed to participate. Similarly, in family PA, 14 positive members (10 females, 4 males) and 17 unaffected family members were enrolled.

The genomic DNA samples of all family members were assessed for linkage to the four reported late-onset FCD loci—*FCD1, FCD2, FCD3,* and *FCD4*—with florescence-labeled STR markers spanning each of the four critical intervals. After assigning genotypes to each person in both families, haplotypes were constructed and were analyzed for segregation with the disease phenotype in their respective families, which suggested that both families are linked to *FCD2*. Next, we calculated two-point LOD scores for both families separately under an autosomal dominant model with 90% penetrance. The inheritance model was guided by estimates of the population prevalence and the observed mode of inheritance for familial late-onset FCD. A two-point LOD of 3.25 was obtained for family PA, whereas family MO yielded a two-point LOD of 3.05 at $\theta = 0$. No positive LOD scores were obtained with alleles for STR makers spanning *FCD1*, *FCD3,* and *FCD4*. Additionally, we interrogated both families for genetic lesions in *SLC4A11* and *TCF8* but did not identify any pathogenic variants.

Previously, we reported three large families mapped to *FCD2* on chromosome 18q21.[9] In conjunction with the two additional families we have since recruited, there are now five large families mapped to *FCD2*. We have been able to investigate the age-severity relationship associated with the *FCD2* disease phenotype in the two newly identified families because of the locality and availability of these families. We acquired retroillumination photographs from 14 affected members of the two families, representing approximately half the total affected members (the remaining family members were unavailable or unwilling to participate). Taken as a whole, nonparticipants were on average 58.7 years of age and had an average Krachmer grading of 3.06 (bilateral averages). Retroillumination photographs allowed for the calculation of total number of guttae for each person.

A total of 29,300 guttae divided among inferotemporal (9,018), superotemporal (8,215), inferonasal (5,919), and superonasal (6,148) are present in five affected persons in family MO. Similarly, in family PA, there are a total of 40,949 guttae divided among inferotemporal (12,666), superotemporal (9,339), inferonasal (10,609), and superonasal (8,335; Table 2). Taken together, families have a total of 70,249 guttae. For all the data collected, there is on average a minor difference (~2.7%) in the guttae distribution between left eye (OS) and right eye (OD) per individual without any bias for OD or OS. We examined the distribution of guttae in the four corneal quadrants for both families combined, and a distribution bias was observed for higher guttae density in the inferotemporal region ($P = 0.016$), as seen previously with an *FCD1*-linked family.[15]

The age-severity relationships of *FCD1*-linked affected persons has been reported previously.[15] *FCD2*-linked families display an exponential trend in severity with age, as was observed in a family linked to *FCD1* (Fig. 2). Using regression analyses, we compared the age-severity relationships of families linked to *FCD1* and *FCD2* (Fig. 2). The regression model suggests that for families linked to *FCD1*, on average the number of guttae increases 1.24 times ($P = 0.001$, 95% CI: (1.11, 1.39)) annually. While for families linked to *FCD2*, the number of guttae increases 1.05 times ($P = 0.02$; 95% CI: 1.01, 1.09) annually. When comparing the age-severity relationships of the two families, *FCD2*-linked persons' annual increase rate of the number of guttae is 84% of the annual increase rate for *FCD1*-linked persons.

Table 2. Representation of Total Number of Guttae for Both *FCD2*-Linked Families and Spatial Distribution in All Quadrants of the Cornea

	Total No. of Guttae	Decimal of Total	Difference vs. Inferotemporal (*P*)
Inferotemporal	21,684	0.30867	—
Superonasal	14,483	0.206167	0.002
Superotemporal	17,554	0.249883	0.007
Inferonasal	16,528	0.235277	0.016

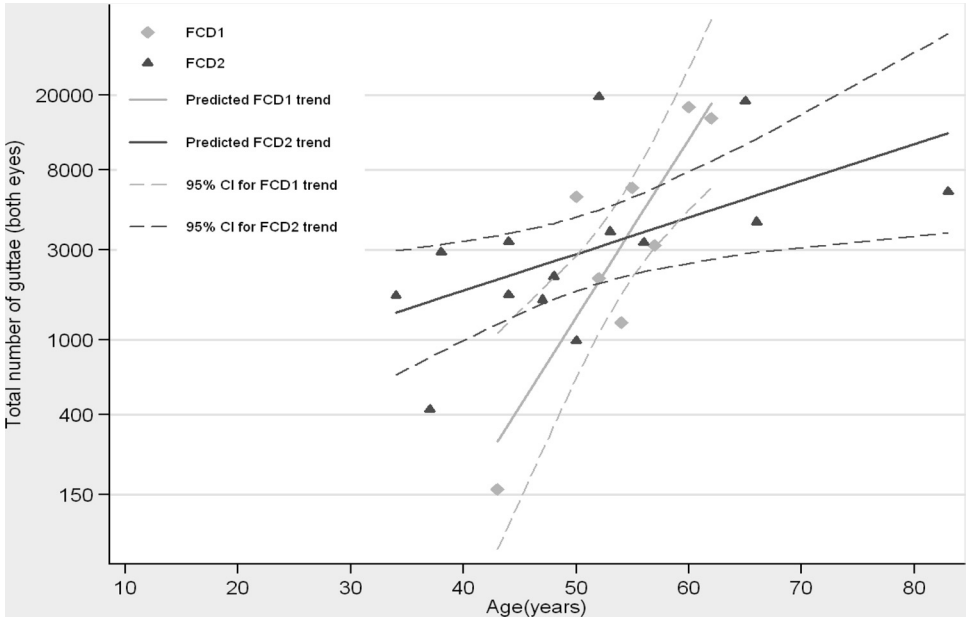

FIGURE 2. Predicted trends and 95% confidence intervals associated with *FCD1* and *FCD2*.

DISCUSSION

We report the age severity relation of Fuchs corneal dystrophy in *FCD2*-linked families using retroillumination photography. We examined two newly recruited families, both of whom map to *FCD2* on chromosome 18q21 with significant two-point LOD scores. Retroillumination photographs were acquired from 14 persons, and guttae in each eye were manually counted. The results suggest that *FCD2*-linked families fit an exponential model for age and severity and show a propensity for higher guttae concentration in the inferotemporal quadrant of the cornea.

Previously, we reported an exponential progression model with an *FCD1*-linked family.[15] In addition, using baseline data, we found that the *FCD1*-linked family also fits an exponential age-severity model. Similar to *FCD1*, families linked to *FCD2* manifest an exponential relationship between age and severity, but the trend is less severe when compared with an *FCD1*-linked family. Interestingly, both *FCD1*- and *FCD2*-linked families share a tendency for higher numbers of inferotemporal guttae.

Previously, we compared the severity of the disease phenotype, measured on a scale proposed by Krachmer et al., with age in affected members of families linked to *FCD1*, *FCD2,* and *FCD3*.[10] Our results suggested that when compared across the same age, *FCD1*-linked affected persons manifest the most severe phenotype, followed by *FCD2* and then by *FCD3*.[10] Here, we have determined the severity of the disease phenotype with retroillumination photography and have compared *FCD1*- and *FCD2*-linked affected persons across age. In accordance with our published results, our data strongly suggest that affected persons harboring the *FCD1* haplotype develop a relatively severe disease phenotype at an earlier age compared with *FCD2*-linked affected persons. However, additional families would be valuable in further verifying that these trends are the property of late-onset FCD loci and not a simple characteristic of these families, whose additional genetic load is unclear at present.

Establishing the age-severity relationship for known FCD loci with retroillumination provides a more precise phenotype/genotype relationship in the number of guttae with age. In contrast to the Krachmer scale, which takes into account only the linear, horizontal central corneal guttae, retroillumination photography documents all four quadrants of the cornea. Recognizing patterns in guttae presentation could more precisely define the disease phenotypes among various genotypes of FCD. Additionally, documentation of disease presentation for each locus may serve as an indicator of disease progression and subsequently help to predict the severity associated with a particular locus.

Acknowledgment

The authors thank all the families for their participation in this study.

References

1. Lorenzetti DW, Uotila MH, Parikh N, Kaufman HE. Central cornea guttata: incidence in the general population. *Am J Ophthalmol.* 1967;64:1155–1158.
2. Krachmer JH, Purcell JJ Jr, Young CW, Bucher KD. Corneal endothelial dystrophy: a study of 64 families. *Arch Ophthalmol.* 1978; 96:2036–2039.
3. Mannis MJ, Holland EJ, Beck RW, et al. Clinical profile and early surgical complications in the Cornea Donor Study. *Cornea.* 2006; 25:164–170.
4. Bergmanson JP, Sheldon TM, Goosey JD. Fuchs' endothelial dystrophy: a fresh look at an aging disease. *Ophthalmic Physiol Opt.* 1999;19:210–222.
5. Vogt A. Weitere Ergebnisse der Spaltlampenmikroskopie des vordern Bulbusabschnittes. *Arch Ophthalmol.* 1921:63–113.
6. Gottsch JD, Zhang C, Sundin OH, Bell WR, Stark WJ, Green WR. Fuchs corneal dystrophy: aberrant collagen distribution in an L450W mutant of the COL8A2 gene. *Invest Ophthalmol Vis Sci.* 2005;46:4504–4511.
7. Gottsch JD, Sundin OH, Liu SH, et al. Inheritance of a novel COL8A2 mutation defines a distinct early-onset subtype of Fuchs corneal dystrophy. *Invest Ophthalmol Vis Sci.* 2005;46:1934–1939.
8. Sundin OH, Jun AS, Broman KW, et al. Linkage of late-onset Fuchs corneal dystrophy to a novel locus at 13pTel-13q12.13. *Invest Ophthalmol Vis Sci.* 2006;47:140–145.
9. Sundin OH, Broman KW, Chang HH, Vito EC, Stark WJ, Gottsch JD. A common locus for late-onset Fuchs corneal dystrophy maps to 18q21.2-q21.32. *Invest Ophthalmol Vis Sci.* 2006;47: 3919–3926.
10. Riazuddin SA, Eghrari AO, Al-Saif A, et al. Linkage of a mild late-onset phenotype of Fuchs corneal dystrophy to a novel locus at 5q33.1-q35.2. *Invest Ophthalmol Vis Sci.* 2009;50:5667–5671.

11. Riazuddin SA, Zaghloul NA, Al-Saif A, et al. Missense mutations in TCF8 cause late-onset Fuchs corneal dystrophy and interact with FCD4 on chromosome 9p. *Am J Hum Genet.* 2010;86:45–53.
12. Krafchak CM, Pawar H, Moroi SE, et al. Mutations in TCF8 cause posterior polymorphous corneal dystrophy and ectopic expression of COL4A3 by corneal endothelial cells. *Am J Hum Genet.* 2005;77:694–708.
13. Vithana EN, Morgan PE, Ramprasad V, et al. SLC4A11 mutations in Fuchs endothelial corneal dystrophy. *Hum Mol Genet.* 2008;17:656–666.
14. Gottsch JD, Sundin OH, Rencs EV, et al. Analysis and documentation of progression of Fuchs corneal dystrophy with retroillumination photography. *Cornea.* 2006;25:485–489.
15. Meadows DN, Eghrari AO, Riazuddin SA, Emmert DG, Katsanis N, Gottsch JD. Progression of Fuchs corneal dystrophy in a family linked to the FCD1 locus. *Invest Ophthalmol Vis Sci.* 2009;50:5662–5666.
16. Lathrop GM, Lalouel JM. Easy calculations of lod scores and genetic risks on small computers 509. *Am J Hum Genet.* 1984;36:460–465.
17. Schaffer AA, Gupta SK, Shriram K, Cottingham RW. Avoiding recomputation in genetic linkage analysis 1669. *Hum Hered.* 1994;44:225–237.
18. Krawetz S, Misener S, eds. *Bioinformatics Methods and Protocols: Methods in Molecular Biology.* Totowa, NJ: Humana Press; 2000:365–386.
19. Rabe-Hesketh S, Skrondal A. *Multilevel and Longitudinal Modeling Using Stata*. College Station, TX: Stata Press. 2005.
20. Hamilton LC. *Statistics with Stata: Updated for Version 9*. North Scituate, MA: Duxbury Press. 2006.